THE ANNALS OF "DUNĂREA DE JOS" UNIVERSITY OF GALAȚI
FASCICLE V, TECHNOLOGIES IN MACHINE BUILDING,
ISSN 1221- 4566

STUDY OF THE GEAR FORMED BY A STAR WHEEL WITH TRAPEZOIDAL PROFILE AND ITS CONJUGATED WORM

Gabriel FRUMUŞANU, Nicolae OANCEA

"Dunărea de Jos" University of Galati, Manufacturing Engineering Department,
gabriel.frumusanu@ugal.ro

ABSTRACT

The paper presents an analysis based on a complementary theorem concerning the enwrapped profiles – the Generating trajectories method, regarding the profile of the cylindrical worm conjugated to a star-wheel having teeth with trapezoidal profile. This type of gear can be met at the so called "single screw compressors" or in transmissions with kinematical purpose, working at low torques. An algorithm dedicated to find the worm profile has been developed. The specific problems of both primary interference and assemblage interference have been addressed. A numerical application for sampling the analytical results application in practice is also included.

Keywords: star wheel – conjugated worm gear, trapezoidal tooth profile, generating trajectories method, worm profile, interference

1. INTRODUCTION

The single screw compressor developed as an alternative solution to twin screw compressor, being capable of high energy efficiency by diminishing losses due to leakage, frictional effects and heat transfer factors [1].

The main components of single screw compressor are the central screw (a cylindrical worm with one or more threads) and two gate rotors (star wheels), located on both sides of the central screw and having at least one tooth in meshing engagement with its threads (Fig. 1).

Fig. 1. *Single screw compressor [2]*

Different profiles of the star-wheel tooth have been proposed [3], while the worm profile is conjugated to the tooth one and can be determined by applying the fundamental theorems concerning the reciprocally-enwrapped surfaces [4, 5].

In this paper, we suggest approaching the worm profiling and the specific interference problems (between worm and star wheel tooth profiles) on the base of a complementary theorem – the generating trajectories method [6, 7]. A profiling algorithm has been developed in the case of the star-wheel with trapezoidal tooth profile. The algorithm has been subsequently implemented in MatLab, the axial profile of the conjugated worm resulting by the coordinates of a set of points. By starting from here, the potential interference problems (primary or assemblage interference) can also be studied.

The next section presents the geometry of the star-wheel with trapezoidal tooth profile. In the third section, the worm axial profile is found, in analytical form, while the fourth deals with worm numerical model. The fifth section addresses to the interference problem, the sixth is dedicated to a numerical application, while the last one is for conclusion.

2. THE STAR WHEEL WITH TRAPEZOIDAL TOOTH PROFILE

Fig. 2 shows the plain profile of the star wheel and the reference systems associated to the rolling centroids of the star-wheel (circle of R_r radius) and of the conjugated worm axial section (straight line, tangent to the circle).

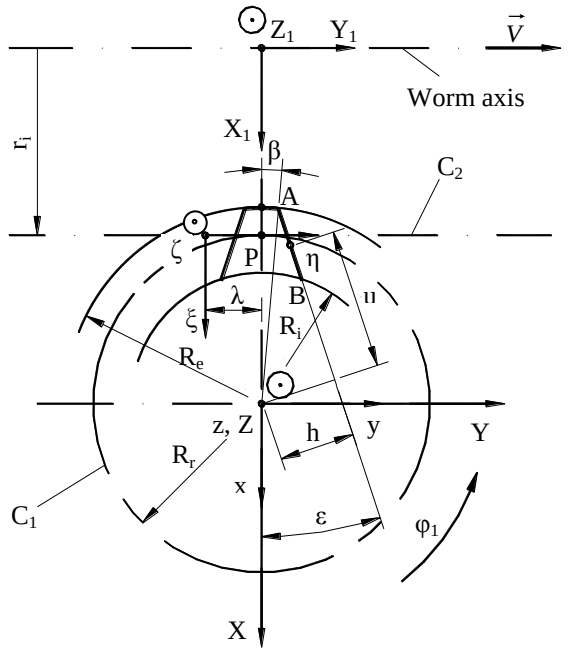

Fig. 2. *Star-wheel profile: the rolling centroids & the reference systems*

We introduce the following denominations:

- C_1, meaning the centroids of R_r radius, attached to the star wheel
- C_2 – the rectilinear centroids attached to worm axial section – the conjugated rack-gear
- *xyz* – global system, attached to star-wheel rotation axis
- *XYZ* – relative system, mobile, moving together with C_1 (hence with the star wheel too)
- $\xi\eta\zeta$ – relative system, mobile, associated to the generator rack-gear
- $X_1Y_1Z_1$ – relative system, mobile, attached to the worm, which has the axis $\vec{V}$ (coincident to Y_1 and the helical parameter *p*.

Hereby, the condition of centroids rolling is:

$$\lambda = R_r \cdot \varphi_1 \tag{1}$$

The tooth flank of star wheel with trapezoidal profile can be analytically expressed as:

$$\overline{AB}\begin{vmatrix} X = -h\sin\varepsilon - u\cos\varepsilon; \\ Y = h\cos\varepsilon - u\sin\varepsilon, \end{vmatrix} \tag{2}$$

with *u* variable. The extreme values of *u* can be determined from the relations:

$$\sqrt{h^2 + u_{min}{}^2} = R_i, \sqrt{h^2 + u_{max}{}^2} = R_e. \tag{3}$$

In relation (3), R_i, R_e and h are constructive parameters, characterizing the geometry of the star wheel tooth.

3. PROFILE OF WORM AXIAL SECTION

The kinematics for generating worm axial section results by composing two motions:

- rotation of C_1 centroid,

$$x = \omega_3^T(\varphi_1)\cdot X \tag{4}$$

- translation of C_2 centroid,

$$\xi = x - a,\ a = \begin{Vmatrix} -R_r \\ -R_r\cdot\varphi_1 \end{Vmatrix}. \tag{5}$$

As a consequence, the relative motion between the mobile systems is:

$$\xi = \omega_3^T(\varphi_1)\cdot X - \begin{Vmatrix} -R_r \\ -R_r\cdot\varphi_1 \end{Vmatrix}. \tag{6}$$

Due to motion (6), the family of $\overline{AB}$ flanks results, into rack-gear reference system, as:

$$\left(\overline{AB}\right)_{\varphi_1}\begin{vmatrix} \xi = \left(-h\sin\varepsilon - u\cos\varepsilon\right)\cos\varphi_1 - \\ \quad -\left(h\cos\varepsilon - u\sin\varepsilon\right)\sin\varphi_1 + R_r; \\ \eta = \left(-h\sin\varepsilon - u\cos\varepsilon\right)\sin\varphi_1 + \\ \quad +\left(h\cos\varepsilon - u\sin\varepsilon\right)\cos\varphi_1 + R_r\cdot\varphi_1. \end{vmatrix} \tag{7}$$

Profiles family envelop (7) is the profile of the generator rack-gear (the conjugated worm's axial section). The enveloping condition will be further determined, according to generating trajectories method. In this purpose, the directional cosines of the normal to *AB* profile (Fig. 2) are firstly calculated:

$$\vec{n}_{AB} = \begin{vmatrix} \vec{i} & \vec{j} & \vec{k} \\ -\cos\varepsilon & -\sin\varepsilon & 0 \\ 0 & 0 & 1 \end{vmatrix} = -\sin\varepsilon\cdot\vec{i} + \cos\varepsilon\cdot\vec{j}. \tag{8}$$

Hereby, the normal in the current point of the tooth flank has the expression:

$$\begin{aligned} \vec{N}_{AB} = &\left(-h\sin\varepsilon - u\cos\varepsilon - k\sin\varepsilon\right)\vec{i} + \\ &+\left(h\cos\varepsilon - u\sin\varepsilon + k\cos\varepsilon\right)\vec{j}, \end{aligned} \tag{9}$$

k meaning a variable scalar.

Then, $\vec{N}_{AB}$ trajectories in its relative motion respect to the rack-gear system result from (6):

$$\left(\vec{N}_{AB}\right)_{\varphi_1}\begin{vmatrix} \xi = \left(-h\sin\varepsilon - u\cos\varepsilon - k\sin\varepsilon\right)\cos\varphi_1 - \\ \quad -\left(h\cos\varepsilon - u\sin\varepsilon + k\cos\varepsilon\right)\sin\varphi_1 + \\ +R_r; \\ \eta = \left(-h\sin\varepsilon - u\cos\varepsilon - k\sin\varepsilon\right)\sin\varphi_1 + \\ \quad +\left(h\cos\varepsilon - u\sin\varepsilon + k\cos\varepsilon\right)\cos\varphi_1 + \\ +R_r\cdot\varphi_1. \end{vmatrix} \tag{10}$$

By imposing to normal family the condition of passing by the gearing pole *P* (the point of tangency between the two centroids, see Fig. 2),

$$P\begin{vmatrix}\xi = 0;\\ \eta = R_r \cdot \varphi_1,\end{vmatrix} \quad (11)$$

from (10) we obtain, by eliminating *k* between the two relations, the enveloping condition:

$$u = R_r \cos(\varepsilon + \varphi_1). \quad (12)$$

The condition (12) associated to the equations of the family (7) determines the axial profile of the conjugated worm (the generator rack-gear of the star wheel), looking in principle like:

$$S_A\begin{vmatrix}\xi = \xi(\varphi_1);\\ \mu = \eta(\varphi_1).\end{vmatrix} \quad (13)$$

Concretely, the rack-gear profile S_A (the worm axial section) will result as a matrix, formed by the coordinates of a given number of points:

$$S_A = \begin{Vmatrix}\xi_1, \eta_1\\ \xi_2, \eta_2\\ \vdots\\ \xi_n, \eta_n\end{Vmatrix}. \quad (14)$$

4. WORM NUMERICAL MODEL

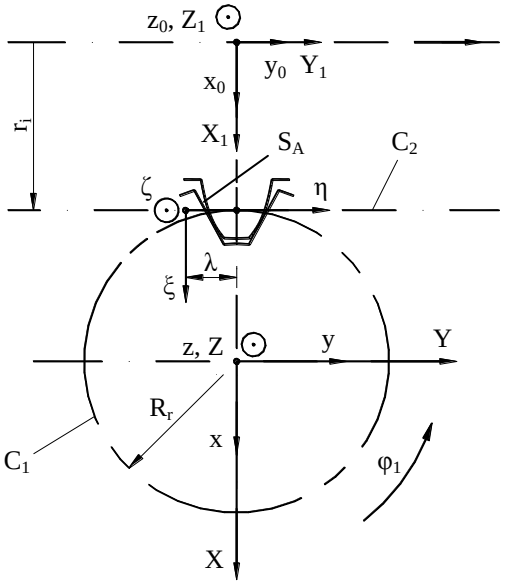

Fig. 3. *The position of the reference systems associated to the worm and to the wheel*

The worm playing the role of central screw can be modelled in numerical form by giving to its axial section (14) a helical motion of $\vec{V}$ axis and *p* helical parameter, identical to the axis and helical parameter of the worm, Fig. 3.

In addition to the reference systems already mentioned in section 2, we also consider $x_0y_0z_0$, meaning a global system attached to worm axis. Its position relative to $\xi\eta\zeta$ system results from

$$x_0 = x - A,\ A = \begin{Vmatrix}-(R_r + r_i)\\ 0\\ 0\end{Vmatrix}, \quad (15)$$

and from (5). Hereby, we have:

$$x_0 = \xi = a - A. \quad (16)$$

If the last transform is applied to the set of points giving worm's axial section (14), then it follows that:

$$\begin{Vmatrix}x_{0j}\\ y_{0j}\\ z_{0j}\end{Vmatrix} = \begin{Vmatrix}\xi_j\\ \eta_j\\ 0\end{Vmatrix} + \begin{Vmatrix}r_i\\ -\lambda\\ 0\end{Vmatrix},\ j = 1,2\ldots n. \quad (17)$$

The rotation of φ_2 angle around worm's axis can is expressed through the equation:

$$x_0 = \omega_2^T(\varphi_2) \cdot X_1. \quad (18)$$

The inverse transform, applied to the set of points giving worm's axial section (17) leads to:

$$X_1 = \omega_2(\varphi_2)\begin{Vmatrix}x_{0j}\\ y_{0j}\\ z_{0j}\end{Vmatrix},\ j = 1,2\ldots n. \quad (19)$$

If we accept that the worm is cylindrical and of *p* parameter, then λ (the parameter measuring rack-gear's translation) must obey to condition:

$$\lambda = p \cdot \varphi_2. \quad (20)$$

Finally, from (19) and (20), after development, the worm equations result, in discrete form, as:

$$S\begin{vmatrix}X_{1j} = (\xi_j + r_i)\cos\varphi_2;\\ Y_{1j} = \eta_j - p \cdot \varphi_2;\\ Z_{1j} = (\xi_j + r_i)\sin\varphi_2,\end{vmatrix} \quad j = 1,2\ldots n. \quad (21)$$

These represent, for φ_2 – discrete, a "solid" formed of points coordinates giving the numerical model of the worm.

Note An analytical form of the worm axial section can also be expressed, from (7) and (12):

$$S_A \begin{cases} \xi = \left[-h\sin\varepsilon - R_r\cos(\varepsilon+\varphi_1)\cos\varepsilon\right]\cos\varphi_1 - \\ \quad -\left[h\cos\varepsilon - R_r\cos(\varepsilon+\varphi_1)\sin\varepsilon\right]\sin\varphi_1 + R_r\,; \\ \eta = \left[-h\sin\varepsilon - R_r\cos(\varepsilon+\varphi_1)\cos\varepsilon\right]\sin\varphi_1 + \\ \quad +\left[h\cos\varepsilon - R_r\cos(\varepsilon+\varphi_1)\sin\varepsilon\right]\cos\varphi_1 + R_r\cdot\varphi_1\,. \end{cases} \quad (22)$$

In this case, the equations of worm peripheral surface result as follows:

$$S \begin{cases} X_1 = (\xi + r_i)\cos\varphi_2\,; \\ Y_1 = \eta - p\cdot\varphi_2\,; \\ Z_1 = (\xi + r_i)\sin\varphi_2\,. \end{cases} \quad (23)$$

5. THE GEAR INTERFERENCE AT ASSEMBLAGE

In reality, the star-wheel has a significant thickness, so its flank is a 3D cylindrical surface. As a consequence, the equations (2) should be replaced by:

$$\overline{AB} \begin{cases} X = -h\sin\varepsilon - u\cos\varepsilon\,; \\ Y = h\cos\varepsilon - u\sin\varepsilon\,; \\ Z = t\,. \end{cases} \quad (24)$$

In the relation from above, *t* means a parameter varying along star-wheel axis.

In assemblage position, the surfaces (23) and (24) might interfere, this being called "interference at assemblage" of the gear. High values of *t* parameter put the gear in the impossibility of functioning.

Through the coordinates transformation ?:

$$\begin{aligned} X_1 &= X + R_r + r_i\,; \\ Y_1 &= Y\,; \\ Z_1 &= Z\,, \end{aligned} \quad (25)$$

the surface of wheel tooth's flank is transposed in the reference system of the worm, enabling to have both surfaces expressed in the same system, so they can be intersected. The interference points position can be found by solving the system:

$$\begin{cases} -h\sin\varepsilon - u\cos\varepsilon + R_r + r_i = (\xi + r_i)\cos\varphi_2\,; \\ h\cos\varepsilon - u\sin\varepsilon = \eta - p\cdot\varphi_2\,; \\ t = -(\xi + r_i)\sin\varphi_2\,. \end{cases} \quad (26)$$

6. NUMERICAL APPLICATION

A numerical application has been developed in MatLab in order to implement the above-presented analytical solution for studying the star wheel – conjugated worm gear.

The input values of the parameters defining the gear geometry (Fig. 2) were the following:

- Wheel tooth foot radius: R_i = 40 mm;
- Wheel tooth head radius: R_e = 45 mm;
- Wheel rolling radius: R_r = 42.5 mm;
- Tooth flank angle: ε = 20º;
- Half-angle at centre corresponding to wheel tooth head: β = 10º;
- Worm rolling radius: r_i = 30 mm;
- Worm helical parameter: $p = 9/\pi$ mm.

The constructive parameter *h* can be calculated (see also Fig. 2) with:

$$h = R_e\sin(\beta + \varepsilon) \quad (24)$$

In the addressed numerical application, according to the above-mentioned values of the gear parameters,

h = 22.5 mm.

First of all, the application determines, by points, the rack-gear profile S_A (the worm axial section), in the form (14). Because of symmetry, only the left flank case has been considered.

In Table 1, there are presented the points' coordinates (computed after considering a 20 points mesh of $[u_{min}, u_{max}]$ interval).

In Fig. 4, the rack-gear profile, obtained by joining 100 points along it, their coordinates being calculated by the application, is represented next to wheel tooth flank profile.

Then, by giving to φ_2 angle, from (23), a discrete variation inside the interval comprised between $-\pi$ and π (in n_{φ_2} = 200 points), with ξ and η calculated according to (22), the application finds the surface *S* of worm's peripheral surface for a turn of the screw. This surface is presented, in graphical form, in Fig. 5.

Table 1. *Worm axial section*

Crt. no.	ξ [mm]	η [mm]
1	1.8910	10.4972
2	1.6163	10.2873
3	1.3426	10.0834
4	1.0702	9.8859
5	0.7996	9.6948
6	0.5310	9.5103
7	0.2648	9.3326
8	0.0015	9.1619
9	-0.2584	8.9984
10	-0.5145	8.8424
11	-0.7660	8.6941
12	-1.0123	8.5538
13	-1.2526	8.4216
14	-1.4859	8.2981
15	-1.7111	8.1834
16	-1.9270	8.0779
17	-2.1320	7.9821
18	-2.3242	7.8964
19	-2.5014	7.8213
20	-2.6608	7.7574

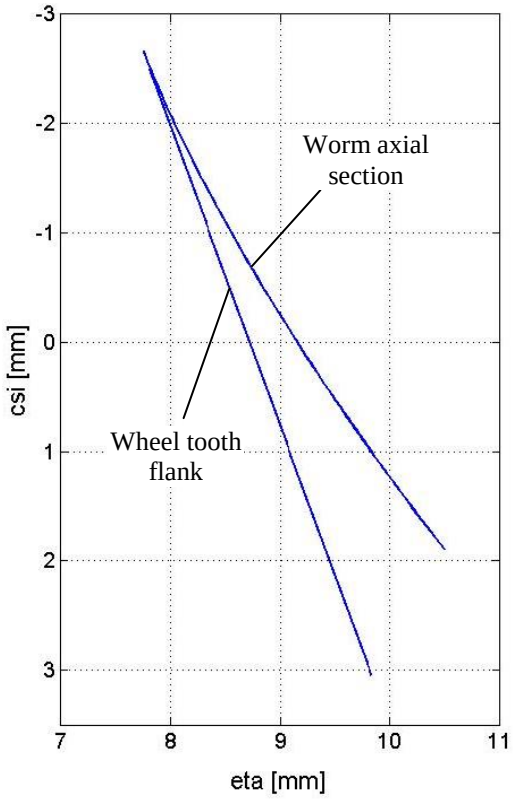

Fig. 4. *Profile of worm axial section*

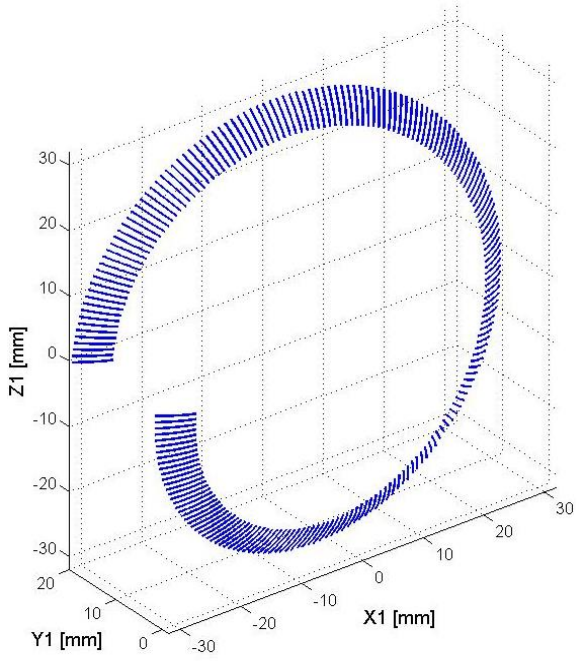

Fig. 5. *Worm peripheral surface S (left flank)*

By numerically solving the system (26), the interference points' coordinates have been found. To this purpose, a discrete variation for t parameter was firstly considered, followed by the determination of the coordinates of the interference point from the plane
$Z_1 = t_k$, $k = 1 \ldots n_t$. Here, a limit value was not imposed for t, although in real cases this exists, being determined by the star wheel width, b, namely:

$$t_{max} = b / 2 . \qquad (25)$$

In Table 2, there are presented the coordinates of the interference points occurring in the addressed numerical application, while in Fig. 6 it is represented the curve resulted after joining these points.

Table 2. *Coordinates of interference points*

Crt. no.	X_1 [mm]	Y_1 [mm]	Z_1 [mm]
1	27.2809	8.4839	0
2	27.3021	8.4915	-0.0136
3	27.3236	8.4992	-0.0273
4	27.3422	8.5059	-0.0410
5	27.3642	8.5140	-0.0547
6	27.3865	8.5223	-0.0685
7	27.4026	8.5280	-0.0822
8	27.4188	8.5338	-0.0960
9	27.4352	8.5397	-0.1098
10	27.4517	8.5456	-0.1236
.....			
947	25.5529	7.8538	-13.0918
948	25.5424	7.8498	-13.1026
949	25.5319	7.8458	-13.1133
950	25.5253	7.8444	-13.1261
951	25.5148	7.8404	-13.1368
952	25.5042	7.8364	-13.1476
953	25.4937	7.8324	-13.1583
954	25.4832	7.8284	-13.1690
955	25.4766	7.8270	-13.1818
956	25.4660	7.8230	-13.1925

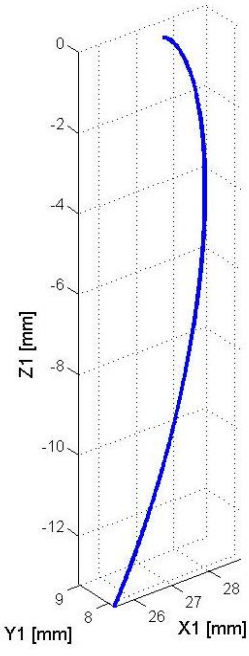

Fig. 6. *The interference curve*

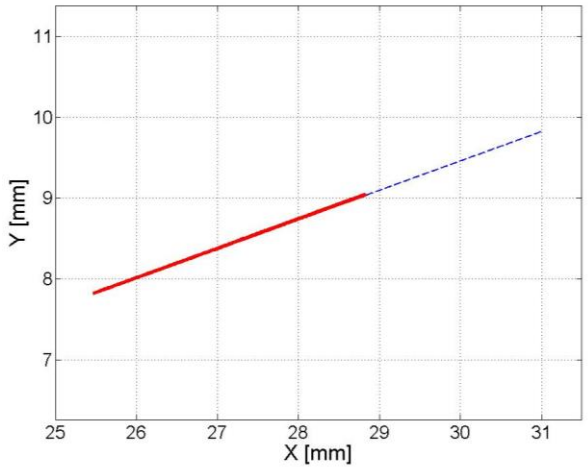

Fig. 7. *Length of wheel tooth flank affected by interference*

The length of wheel tooth flank affected by the interference at assembly phenomenon can be noticed if projecting the points of intersection between the two surfaces (wheel tooth flank and worm helix) on *XY* plane, next to the segment representing the tooth flank profile. In Fig. 7, the interference points' locus is represented with continuous, thicker line, while the rest of the tooth flank is in dashed line.

As it can be easily observed, a significant part of tooth flank is concerned by the interference at assembly.

The solution for avoiding severe malfunctions in gear functioning is to adopt as smaller as possible values for wheel width *b* and/or to use modified profiles for tooth flank.

7. CONCLUSION

In this paper, an analysis of the gear formed by a star wheel with tooth trapezoidal profile and its conjugated helical worm is presented. Gear geometry has been studied on the base of a complementary theorem concerning the enwrapped profiles – the Generating trajectories method. After defining the wheel tooth flank profile by appropriate parameters, the profile of the worm axial section has been analytically determined. A solution for building the worm numerical model has been consequently developed, in order to enable the finding of the points where wheel tooth and worm surfaces do intersect. The numerical simulation proved the correctness of the deducted equations and the utility of the solution for studying the interference at assemblage.

REFERENCES

[1] *Single screw compressors*, available at http://www.emersonclimate.com
[2] *Compressor Airend & Rebuilts*, available at http://www.nirvatech.com/products.php?pageID=9&catID=29&productID=27
[3] G. Frumuşanu, V. Teodor, S. Totolici, N. Oancea, *The interference at the assemblage of cylindrical worm – star wheel gear*, Proceedings in Manufacturing Systems, 2016, in press.
[4] F.L. Litvin, *Theory of gearing*, NASA, Scientific and Technical information Division, Washington DC, 1984.
[5] S.P. Radzevich, *Kinematics Geometry of Surface Machining*, CRC Press, London, 2008.
[6] N. Oancea, *Surfaces generation through winding, vol. I – III*, Galati University Press, Galați, 2004.
[7] N. Baroiu, V. Teodor, N. Oancea, *A new form of in plane trajectories theorem. Generation with rotary cutters*, Bulletin of the Polytechnic Inst. of Iași, Tome LXI (LV), Fasc. 3, 2015, pp. 29–36.